

# Journal of Mechanics of Materials and Structures

**APPLICATION OF THE HYBRID COMPLEX VARIABLE METHOD TO  
THE ANALYSIS OF A CRACK AT A PIEZOELECTRIC-METAL INTERFACE**

Volodymyr Govorukha and Marc Kamlah

**Volume 13, No. 4**

**July 2018**



# APPLICATION OF THE HYBRID COMPLEX VARIABLE METHOD TO THE ANALYSIS OF A CRACK AT A PIEZOELECTRIC-METAL INTERFACE

VOLODYMYR GOVORUKHA AND MARC KAMLAH

A plane strain problem for an electrically conducting interface crack between linear transversely isotropic piezoelectric and isotropic elastic conductor materials under remote mechanical loading is considered. The attention is focused on a hybrid complex variable method which combines the Stroh formalism for piezoelectric materials with the Muskhelishvili formalism for conducting isotropic elastic materials. This method is illustrated in detail for the open crack model and the contact zone crack model. Using special presentations of mechanical quantities via sectionally analytic functions, a combined Dirichlet–Riemann and Hilbert boundary value problem is formulated and solved analytically. Stress intensity factors as well as the crack tip energy release rate are found in a clear analytical form. Furthermore, transcendental equations for the determination of the realistic contact zone length and the location of the first interpenetration point have been obtained. A significant influence of the external mechanical loading on the crack opening and the stresses as well as the contact zone and interpenetration region lengths is observed. The dependencies of the mentioned values on the intensities of the mechanical loading are presented in tables and associated diagrams.

## 1. Introduction

With the rapid development of modern industry, piezoelectric-metal composites have been widely used in various electromechanical devices. Due to excellent piezoelectric effects as well as good mechanical properties, these composites have become attractive candidates for use in transducers and actuators for vibration control and biomedical imaging applications [Pritchard et al. 2001]. What is even more common, piezoelectric-metal bimetals have an apparent application in any kind of piezoelectric sensors and transducers, where metal electrodes are always placed on piezoelectric material surfaces to introduce high applied electric fields. However, various defects may occur on the interface of the metal and piezoelectric phases due to flaws during manufacturing, impact, cooling or other unexpected reasons. These defects cause geometric, electric and mechanical discontinuities and thus induce strong stress and electric field concentrations, which may induce crack initiation and crack growth, eventually causing fracture and failure. Therefore, it is important to understand and be able to analyze the fracture characteristics of piezoelectric-metal structures so that reliable service life predictions of the pertinent devices can be conducted.

The earliest research on this topic appears to have been done by Kudriavtsev et al. [1975a; 1975b], who modeled an interface crack between a piezoelectric ceramic and an elastic isotropic conductor as rectilinear and axisymmetric, respectively. Liu and Hsia [2003] provided a result for a double edged crack in such a bimaterial under in-plane electric loading. Based on the integral transformation technique,

*Keywords:* Piezoelectric-metal joint, complex variable method, electrically conducting interface crack, contact zone.

Parton [1976] and Bakirov [2004] studied the plane problem of a crack on a piezoelectric-metal interface, in which the axis of axisymmetry of the transversely isotropic piezoelectric materials is normal to the interface and a normal homogeneous tensile loading is applied at infinity. As presented by Bakirov and Kim [2009], the plane strain problem of a crack on an interface between an isotropic elastic conductor and a transversely isotropic piezoelectric material was reduced to the boundary equations on the interface, which make it possible to calculate the crack tip energy release rate with respect to the distribution of the loading applied to the crack surfaces. A more detailed review of the interface crack problem investigation in piezoelectric-metal composites was presented in the review paper by Govorukha et al. [2016].

Since piezoelectric ceramics and metals are two different kinds of solids, especially concerning electronic transport, it is quite difficult to combine their constitutive equations in an interface crack analysis. For convenience, Ou and Chen [2004] and Li and Chen [2007; 2009] assumed that the metal phase could be considered as a special piezoelectric material with extremely large permittivity and extremely small piezoelectricity and in this way used the extended Stroh formalism to treat this interface crack problem. Although a nonpiezoelectric isotropic elastic material can be treated as a special case of piezoelectric materials with vanishing piezoelectric constants, the well-known Stroh formalism, on which almost all of the existing works on interface cracks in piezoelectric media have been based, breaks down or becomes complicated in the degenerate case of isotropic elastic materials due to the appearance of multiple eigenvalues [Ting and Chou 1981]. In order to eliminate this discrepancy, a hybrid complex variable method was proposed by Ru [2008], in which the isotropic elastic material was handled with the convenient and powerful Muskhelishvili formalism while the piezoelectric material was analyzed with the Stroh formalism. This method was illustrated for an insulating interface crack between a piezoelectric half-plane and an isotropic elastic half-plane.

It should be noted that most of the above-mentioned solutions for interface cracks in piezoelectric-metal composites have oscillatory singularities, as in the case of elasticity [Williams 1959], which causes the overlapping of crack faces, a physically unreasonable phenomenon. To correct this shortcoming, Comninou [1977] developed a contact zone model for a crack between two nonpiezoelectric materials. On the basis of this model, a numerical analysis of an interface crack between a piezoelectric ceramic and an elastic isotropic conductor has been performed by Govorukha and Loboda [2000]. However an analytical investigation of an interface crack with contact zones in a piezoelectric-metal bimaterial is unknown, at least to the authors of this paper.

In the present paper a closed-form solution for a conducting interface crack between a piezoelectric half-plane and a conducting isotropic elastic half-plane is obtained with the use of hybrid complex variable method. The open crack model and the contact zone crack model are utilized. A significant influence of the external mechanical loading on the crack opening, stresses as well as the contact zone and interpenetration region lengths is demonstrated.

## 2. Basic equations

The constitutive and equilibrium equations for a linear piezoelectric material in the absence of body forces and free charges can be represented in the form [Pak 1992]

$$\prod_{mJ} = E_{mJKl} V_{K,l}, \quad (1)$$

$$\prod_{mJ,m} = 0, \tag{2}$$

where

$$V_K = \begin{cases} u_k, & K = 1, 2, 3, \\ \varphi, & K = 4, \end{cases} \quad \prod_{mJ} = \begin{cases} \sigma_{mj}, & m, J = 1, 2, 3, \\ D_m, & m = 1, 2, 3; J = 4, \end{cases}$$

$$E_{mJKl} = \begin{cases} c_{mjkl}, & m, J, K, l = 1, 2, 3, \\ e_{lmj}, & m, J, l = 1, 2, 3; K = 4, \\ e_{mkl}, & m, K, l = 1, 2, 3; J = 4, \\ -\varepsilon_{ml}, & m, l = 1, 2, 3; J, K = 4. \end{cases}$$

Here,  $u_k$ ,  $\varphi$ ,  $\sigma_{mj}$ , and  $D_m$  are the elastic displacements, electric potential, stresses, and electric displacements, while  $c_{mjkl}$ ,  $e_{mjkl}$ , and  $\varepsilon_{mj}$  are the elastic, piezoelectric, and dielectric constants, respectively. Lower case subscripts range from 1 to 3, upper case subscripts range from 1 to 4, and summation over repeated subscripts is implied. The subscript comma denotes partial derivative with respect to the Cartesian coordinates. In addition, the electric field  $E_m$  is related to the electric potential  $\varphi$  by

$$E_m = -\varphi_{,m}.$$

For a two-dimensional problems in which  $u_k$  and  $\varphi$  depend on  $x_1$  and  $x_3$  only, a general solution of (1), (2) according to the method originally proposed by Eshelby et al. [1953] and used by Stroh [1958] can be written as

$$V = \mathbf{A}f(z) + \overline{\mathbf{A}}\overline{f(z)}, \tag{3}$$

$$t = \mathbf{B}f'(z) + \overline{\mathbf{B}}\overline{f'(z)}, \tag{4}$$

where  $V = [u_1, u_2, u_3, \varphi]^T$ ,  $t = [\sigma_{13}, \sigma_{23}, \sigma_{33}, D_3]^T$ , and  $f(z)$  consists of four arbitrary analytic functions of the respective variables  $z_\alpha = x_1 + p_\alpha x_3$  ( $\alpha = 1, 2, 3, 4$ ) as

$$f(z) = [f_1(z), f_2(z_2), f_3(z_3), f_4(z_4)]^T.$$

Matrices  $\mathbf{A}$  and  $\mathbf{B}$  are defined by the material constants, and  $p_\alpha$  are four distinct complex roots with positive imaginary parts of the characteristic equation described by Suo et al. [1992]. Here and afterwards, the superscript  $T$  denotes transposition and the overbar stands for the complex conjugate.

In this paper, we consider transversely isotropic piezoelectric materials poled in the  $x_3$ -direction. In this case, the displacement  $u_2$  decouples in the  $(x_1, x_3)$ -plane from  $(u_1, u_3, \varphi)$ . Because of the simplicity of the  $u_2$ -determination our attention will be devoted to the in-plane problem which is characterized by the displacements  $u_1, u_3$  and the electric potential  $\varphi$ . Thus, the second row and the second column will be deleted from all matrices in (3) and (4).

In the case of the plane problems for the isotropic elastic materials, the stresses and associated elastic displacements can be expressed in terms of the Muskhelishvili complex potentials [1953]  $\phi(z)$  and  $\psi(z)$ :

$$2\mu(u_1 - iu_3) = \kappa\overline{\phi(z)} - \bar{z}\phi'(z) - \psi(z),$$

$$\sigma_{33} + i\sigma_{13} = \phi'(z) + \overline{\phi'(z)} + \bar{z}\phi''(z) + \psi'(z),$$

where  $\kappa = 3 - 4\nu$  for plane strain and  $\kappa = (3 - \nu)/(1 + \nu)$  for plane stress, and  $\mu$  and  $\nu$  are the shear modulus and Poisson’s ratio, respectively.

Introducing new analytic functions by the formulas

$$\Psi(z) = \bar{z}\phi''(z) + \psi'(z), \quad \Phi(z) = \phi'(z),$$

one can write,

$$2\mu(u'_1 - iu'_3) = \kappa\overline{\Phi(z)} - \Phi(z) - \Psi(z), \tag{5}$$

$$\sigma_{33} + i\sigma_{13} = \Phi(z) + \overline{\Phi(z)} + \Psi(z). \tag{6}$$

The attention is focused in the following on a hybrid complex variable method which combines the Stroh formalism of the piezoelectric materials with the Muskhelishvili formalism of the conducting isotropic elastic materials (such as metal).

### 3. Complex function representation for the stresses and displacement jumps at the interface

In this section, we develop as a major novelty expressions by which the solution of various mixed boundary conditions at the interface, i.e., different models for cracks between a piezoelectric and a metal, can be obtained. Consider a bimaterial composition, where the piezoelectric phase occupies the upper half-plane ( $x_3 \geq 0$ ) and the metal phase occupies the lower half-plane ( $x_3 \leq 0$ ). We assume, that the stresses and the tangential component of the electric field are continuous across the whole bimaterial interface. The part of the interface which is mechanically bounded is denoted by  $L$ . Then, the boundary conditions at the interface  $x_3 = 0$  are

$$E_1^\pm(x_1, 0) = 0 \quad \text{for } x_1 \in (-\infty, \infty), \tag{7}$$

$$\sigma_{33}^+(x_1, 0) + i\sigma_{13}^+(x_1, 0) = \sigma_{33}^-(x_1, 0) + i\sigma_{13}^-(x_1, 0) \quad \text{for } x_1 \in (-\infty, \infty), \tag{8}$$

$$u_1^+(x_1, 0) - iu_3^+(x_1, 0) = u_1^-(x_1, 0) - iu_3^-(x_1, 0) \quad \text{for } x_1 \in L, \tag{9}$$

where the superscripts “+” and “-” indicate the limit values takes from the upper and the lower half-planes, respectively.

It should be noted that, due to the compatibility conditions at the bonded interface, the respective uniform remote loadings given in the two half-planes must be compatible, in order to give rise to uniform stress and electric fields in the absence of the interface crack. In particular, the component  $E_1^\infty$  of remote uniform electric field parallel to the interface in the upper half-plane must be zero, because it must be compatible with the vanishing tangential electric field of the lower half-plane along the bonded interface.

The electro-elastic field in the upper half-plane is described by the Stroh formalism and given in terms of the three functions  $f_k(z_k)$  of the respective variables  $z_k$  ( $k = 1, 3, 4$ ), while the elastic field in the lower half-plane is described by the Muskhelishvili formalism and given in terms of the two functions  $\Phi(z)$  and  $\Psi(z)$  of the single complex variable  $z$ . Thus, the problem is to determine the three analytic functions  $f_k(z_k)$  in the upper half-plane and two analytic functions  $\Phi(z)$  and  $\Psi(z)$  in the lower half-plane.

Let us define three analytic functions of the single complex variable  $z$  in the upper half-plane, in terms of the functions  $f_k(z_k)$  as

$$\mathbf{g}(z) = \mathbf{A}\mathbf{f}'(z), \tag{10}$$

where  $\mathbf{g}(z) = [g_1(z), g_3(z), g_4(z)]^T$ .

Using relation (10), the expressions (3) and (4) can be represented in the form

$$\mathbf{V}' = \mathbf{g}(z) + \overline{\mathbf{g}(z)}, \tag{11}$$

$$\mathbf{t} = \mathbf{D}\mathbf{g}(z) + \overline{\mathbf{D}\mathbf{g}(z)}, \tag{12}$$

where  $\mathbf{D} = i\mathbf{Y}^{-1}$ ,  $\mathbf{Y} = i\mathbf{A}\mathbf{B}^{-1}$ .

In this paper, as defined before, we consider transversely isotropic piezoelectric materials of the symmetry class 6 mm poled in the  $x_3$ -direction which have an essential practical significance. For this case, the matrix  $\mathbf{D}$  has the form

$$\mathbf{D} = \begin{bmatrix} id_{11} & d_{13} & d_{14} \\ d_{31} & id_{33} & id_{34} \\ d_{41} & id_{43} & id_{44} \end{bmatrix},$$

where all  $d_{ij}$  are real and  $d_{31} = -d_{13}$ ,  $d_{41} = -d_{14}$ ,  $d_{43} = d_{34}$  hold true.

Further, the boundary condition (7) along the whole bimaterial interface and the condition  $E_1^\infty = 0$  at infinity give

$$g_4(z) \equiv 0, \quad x_3 \geq 0.$$

In view of the interface conditions (8) and the relations (6) and (12), the continuity of mechanical tractions along the whole real axis gives

$$q_{11}g_1^+(x_1) + q_{12}\overline{g_1^+(x_1)} + iq_{21}g_3^+(x_1) + iq_{22}\overline{g_3^+(x_1)} = \Phi^-(x_1) + \overline{\Phi^-(x_1)} + \Psi^-(x_1),$$

which can be rewritten as

$$q_{11}g_1^+(x_1) + iq_{21}g_3^+(x_1) - \overline{\Phi^+(x_1)} = \Phi^-(x_1) + \Psi^-(x_1) - q_{12}\overline{g_1^-(x_1)} - iq_{22}\overline{g_3^-(x_1)}, \quad x_1 \in (-\infty, \infty), \tag{13}$$

where  $q_{11} = d_{31} - d_{11}$ ,  $q_{12} = d_{31} + d_{11}$ ,  $q_{21} = d_{13} + d_{33}$ ,  $q_{22} = d_{13} - d_{33}$ .

The left-hand side of (13) is the boundary value of a function analytic in the upper half-plane, and the right-hand side is the boundary value of another function analytic in the lower half-plane. Hence, both functions are equal to a function defined as

$$M(z) = \begin{cases} q_{11}g_1(z) + iq_{21}g_3(z) - \overline{\Phi}(z) & \text{for } x_3 > 0, \\ \Phi(z) + \Psi(z) - q_{12}\overline{g_1}(z) - iq_{22}\overline{g_3}(z) & \text{for } x_3 < 0, \end{cases} \tag{14}$$

which is analytic in the whole plane.

Taking into account that the stresses are bounded at infinity, it follows that  $M(z)|_{z \rightarrow \infty} = M^{(0)} = \text{const.}$  But according to Liouville's theorem, this means that  $M(z) = M^{(0)}$  holds true in the whole plane. Because  $g_1(z)$ ,  $g_3(z)$ ,  $\Phi(z)$ , and  $\Psi(z)$  are arbitrary functions, without loss of generality, one can choose  $M^{(0)} = 0$ . Thus, Equation (14) leads to

$$\begin{aligned} q_{11}g_1(z) + iq_{21}g_3(z) - \overline{\Phi}(z) &= 0, & x_3 > 0, \\ \Phi(z) + \Psi(z) - q_{12}\overline{g_1}(z) - iq_{22}\overline{g_3}(z) &= 0, & x_3 < 0, \end{aligned}$$

and then

$$\begin{aligned} iq_{21}g_3(z) &= -q_{11}g_1(z) + \overline{\Phi}(z), & x_3 > 0, \\ q_{21}\Psi(z) &= (q_{12}q_{21} + q_{11}q_{22})\overline{g_1}(z) - (q_{21} + q_{22})\Phi(z), & x_3 < 0. \end{aligned} \tag{15}$$

Hence, the problem is reduced to the determination of the two functions:  $g_1(z)$  in the upper half-plane and  $\Phi(z)$  in the lower half-plane.

Now taking the derivatives of both sides in the interface condition (9) and using the relations (5) and (11) we obtain

$$g_1^+(x_1) - i g_3^+(x_1) - \frac{\kappa}{2\mu} \bar{\Phi}^+(x_1) = -\bar{g}_1^-(x_1) + i \bar{g}_3^-(x_1) - \frac{1}{2\mu} \Phi^-(x_1) - \frac{1}{2\mu} \Psi^-(x_1), \quad x_1 \in L. \quad (16)$$

Continuity of the displacement across the bonded interface, as inferred from (16), implies that a function defined as

$$\Omega(z) = \begin{cases} g_1(z) - i g_3(z) - (\kappa/2\mu)\bar{\Phi}(z) & \text{for } x_3 > 0, \\ -\bar{g}_1(z) + i \bar{g}_3(z) - (1/2\mu)\Phi(z) - (1/2\mu)\Psi(z) & \text{for } x_3 < 0, \end{cases}$$

is analytic in the whole plane with a cut along  $(-\infty, \infty) \setminus L$  and tends to a constant as  $|z| \rightarrow \infty$ .

Thus,  $g_1(z)$  and  $\Phi(z)$  can be expressed via  $\Omega(z)$  as

$$g_1(z) = p_{11}\Omega(z) + p_{12}\bar{\Phi}(z), \quad x_3 > 0, \quad \Phi(z) = p_{21}\Omega(z) + p_{22}\bar{\Phi}(z), \quad x_3 < 0, \quad (17)$$

where

$$p_{11} = \frac{2\mu}{\Delta}(q_{22} - 2\mu), \quad p_{12} = \frac{2\mu}{\Delta}(2\mu + \kappa q_{21}), \quad p_{21} = \frac{4\mu^2}{\Delta}(q_{11} + q_{21}), \\ p_{22} = \frac{2\mu}{\Delta}[2\mu(q_{21} - q_{11}) + q_{12}q_{21} + q_{11}q_{22}], \quad \Delta = (2\mu - \kappa q_{11})(q_{22} - 2\mu) - (2\mu + \kappa q_{21})(q_{12} + 2\mu).$$

Substituting (15) and (17) into (6), we may express the stresses on the whole interface in terms of the single function  $\Phi(z)$ :

$$\begin{aligned} \sigma_{33}(x_1, 0) + i\sigma_{13}(x_1, 0) &= s_{11}\Omega^+(x_1) + s_{12}\bar{\Phi}^+(x_1) + s_{21}\Omega^-(x_1) + s_{22}\bar{\Phi}^-(x_1), \\ \sigma_{33}(x_1, 0) - i\sigma_{13}(x_1, 0) &= s_{11}\bar{\Phi}^-(x_1) + s_{12}\Omega^-(x_1) + s_{21}\bar{\Phi}^+(x_1) + s_{22}\Omega^+(x_1), \end{aligned} \quad (18)$$

where  $s_{11} = p_{22}$ ,  $s_{12} = p_{21}$ ,  $s_{21} = p_{12}q_{12} + q_{22}(p_{12}q_{11} - p_{21})/q_{21}$ ,  $s_{22} = p_{21}$ . It should be noted that the same expressions of the stresses can be found from relation (12).

Similarly, using (5) and (11), we may evaluate the derivatives of the displacement jumps and find

$$\begin{aligned} \langle u'_1(x_1) \rangle - i \langle u'_3(x_1) \rangle &= \Omega^+(x_1) - \Omega^-(x_1), \\ \langle u'_1(x) \rangle + i \langle u'_3(x_1) \rangle &= \bar{\Phi}^-(x_1) - \bar{\Phi}^+(x_1). \end{aligned} \quad (19)$$

Here and afterwards the brackets  $\langle \dots \rangle$  denote the jump of the corresponding function over bimaterial interface.

Introducing the new functions

$$F_j(z) = \frac{s_{11} + \alpha_j s_{22}}{s_{11} - s_{12} + \alpha_j (s_{22} - s_{21})} \left\{ \Omega(z) + \frac{s_{12} + \alpha_j s_{21}}{s_{11} + \alpha_j s_{22}} \bar{\Phi}(z) \right\}, \quad (20)$$

having the same properties as  $\Phi(z)$ , and combining the first and second equation of (18) one can write

$$\sigma_{33}(x_1, 0) + im_j \sigma_{13}(x_1, 0) = t_j [F_j^+(x_1) + \gamma_j F_j^-(x_1)], \quad (21)$$

where  $\alpha_j$  are the roots of the quadratic equation

$$\frac{s_{12} + \alpha s_{21}}{s_{11} + \alpha s_{22}} = \frac{s_{22} + \alpha s_{11}}{s_{21} + \alpha s_{12}},$$

and

$$m_j = \frac{1 - \alpha_j}{1 + \alpha_j}, \quad \gamma_j = \frac{s_{21} + \alpha_j s_{12}}{s_{11} + \alpha_j s_{22}}, \quad t_j = \frac{s_{11} - s_{12} + \alpha_j (s_{22} - s_{21})}{1 + \alpha_j}, \quad j = 1, 2.$$

On the other hand, (19) and (20) lead to the expression for the derivatives of the displacement jumps

$$\langle u'_1(x_1) \rangle + i s_j \langle u'_3(x_1) \rangle = F_j^+(x_1) - F_j^-(x_1), \tag{22}$$

where  $s_{1,2} = -m_{1,2}$ . Numerical analysis shows that the constants  $\alpha_j, m_j, \gamma_j, t_j$  are real, and besides  $\gamma_2 = 1/\gamma_1$  holds true.

The expressions (21) and (22) play an important role in the following analysis because by means of these expressions the problems of linear relationship for various mixed boundary conditions at the interface can be formulated.

#### 4. Open crack model

Consider now the same bimaterial as in the previous chapter and assume that an electrically conducting interface crack is situated in the region  $-b \leq x_1 \leq b, x_3 = 0$  (Figure 1). Taking into account that the stress intensity factors and the energy release rate for an electrically conducting interface crack depend on the material properties and the applied mechanical loads, but not on the applied electric loads [Zhang and Gao 2004], we pay our attention to the influence of the external mechanical loading only. Therefore, it is assumed that the half-planes are loaded at infinity with uniform stresses  $\sigma_{33}^{(j)} = \sigma_{33}^\infty, \sigma_{13}^{(j)} = \sigma_{13}^\infty$ , and  $\sigma_{11}^{(j)} = (\sigma_{11}^\infty)_j$  which satisfy the continuity conditions at the interface ( $j = 1$  stands for the upper half-plane and  $j = 2$  for the lower one). Because the load does not depend on the coordinate  $x_2$ , the plane strain problem in the  $(x_1, x_3)$ -plane can be considered. The open crack model based upon the initial assumption that the crack is completely open is employed in the following analysis.

For a traction- and charge-free electrically conducting crack, the continuity and boundary conditions at the interface  $x_3 = 0$  are

$$\langle \sigma_{13}(x_1) \rangle = 0, \quad \langle \sigma_{33}(x_1) \rangle = 0, \quad E_1^\pm(x_1, 0) = 0 \quad \text{for } x_1 \in (-\infty, \infty), \tag{23}$$

$$\langle u_1(x_1) \rangle = 0, \quad \langle u_3(x_1) \rangle = 0 \quad \text{for } x_1 \notin (-b, b), \tag{24}$$

$$\sigma_{13}^\pm(x_1, 0) = 0, \quad \sigma_{33}^\pm(x_1, 0) = 0 \quad \text{for } x_1 \in (-b, b). \tag{25}$$

The stress components and the derivatives of the displacement jumps at the bimaterial interface can be represented by means of the expressions (21) and (22), respectively. Due to the method of construction of these expressions, they automatically satisfy the boundary conditions (23) and (24). To satisfy additionally the boundary conditions (25), the homogeneous Hilbert problem

$$F_j^+(x_1) + \gamma_j F_j^-(x_1) = 0, \quad x_1 \in (-b, b), \tag{26}$$

by using expression (21) arises [Muskhelishvili 1953]. Taking into account that for  $x_1 \notin (-b, b)$  the relation  $F_j^+(x_1) = F_j^-(x_1)$  is valid, by use of (21) and the prescribed remote mechanical loads the

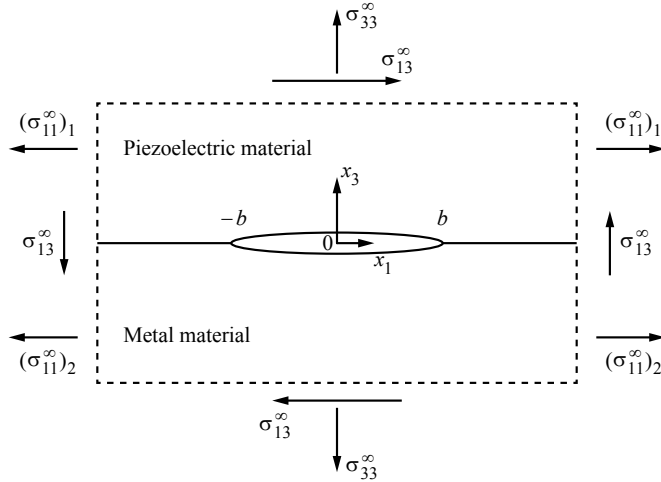


**Figure 1.** An open interface crack subject to remote uniform mechanical loading.

conditions at infinity for the functions  $F_j(z)$  can be written as

$$F_j(z)|_{z \rightarrow \infty} = \frac{\sigma_{33}^\infty + im_j \sigma_{13}^\infty}{t_j(1 + \gamma_j)}. \tag{27}$$

By applying the relation  $\gamma_2 = 1/\gamma_1$ , the solution of this problem for  $j = 2$  can be obtained from the associated solution for  $j = 1$ . Therefore, in the following our attention will be focused only to the case  $j = 1$ . According to the results by Muskhelishvili [1953] the most general solution of the homogeneous Hilbert problem (26), analytic at infinity, has the form

$$F_1(z) = (z + b)^{-1/2+i\varepsilon_1} (z - b)^{-1/2-i\varepsilon_1} P(z),$$

where  $\varepsilon_1 = (\ln \gamma_1)/2\pi$ ,  $P(z) = C_1 z + C_0$ , and  $C_0, C_1$  are arbitrary constants.

Further, by means of the condition at infinity (27) and the condition of the single-valuedness of the displacements, which due to (22) can be written as

$$\int_{-b}^b \{F_1^+(x_1) - F_1^-(x_1)\} dx_1 = 0,$$

the expressions

$$C_0 = \frac{-il\varepsilon_1(\sigma_{33}^\infty + im_1\sigma_{13}^\infty)}{t_1(1 + \gamma_1)}, \quad C_1 = \frac{\sigma_{33}^\infty + im_1\sigma_{13}^\infty}{t_1(1 + \gamma_1)}$$

for the unknown coefficients of the polynomial  $P(z)$  are found and the function  $F_1(z)$  can be represented in the form

$$F_1(z) = \frac{\sigma_{33}^\infty + im_1\sigma_{13}^\infty}{t_1(1 + \gamma_1)} (z + b)^{-1/2+i\varepsilon_1} (z - b)^{-1/2-i\varepsilon_1} (z - il\varepsilon_1), \tag{28}$$

where  $l = 2b$  is the crack length.

Substituting (28) into (21), we get the expressions

$$\sigma_{33}(x_1, 0) + im_1\sigma_{13}(x_1, 0) = \frac{\sigma_{33}^\infty + im_1\sigma_{13}^\infty}{\sqrt{(x_1 + b)(x_1 - b)}}(x_1 - il\varepsilon_1) \left[ \frac{x_1 + b}{x_1 - b} \right]^{i\varepsilon_1} \tag{29}$$

for the stresses at the bonded part  $x_1 > b$  of the bimaterial interface. Substituting (28) into (22), the expressions for the derivatives of the crack face’s displacement jumps can be written as

$$\langle u'_1(x_1) \rangle + is_1 \langle u'_3(x_1) \rangle = \frac{\sigma_{33}^\infty + im_1\sigma_{13}^\infty}{it_1\sqrt{\gamma_1}(x_1 + b)(b - x_1)}(x_1 - il\varepsilon_1) \left[ \frac{x_1 + b}{b - x_1} \right]^{i\varepsilon_1}. \tag{30}$$

Integrating the last expression, one obtains

$$\langle u_1(x_1) \rangle + is_1 \langle u_3(x_1) \rangle = \frac{i(\sigma_{33}^\infty + im_1\sigma_{13}^\infty)}{t_1\sqrt{\gamma_1}}\sqrt{(x_1 + b)(b - x_1)} \left[ \frac{x_1 + b}{b - x_1} \right]^{i\varepsilon_1}. \tag{31}$$

Introducing similarly to Rice [1988] the complex stress intensity factor (SIF) is

$$K_1 + im_1K_2 = \lim_{x_1 \rightarrow b+0} \sqrt{2\pi(x_1 - b)} [\sigma_{33}(x_1, 0) + im_1\sigma_{13}(x_1, 0)](x_1 - b)^{i\varepsilon_1 l - i\varepsilon_1}$$

at the right crack tip, associated to the crack length and using (29) one arrives at the expression for the conjugating SIF:

$$K_1 - im_1K_2 = \sqrt{\frac{1}{2}\pi l}(1 + 2i\varepsilon_1)(\sigma_{33}^\infty - im_1\sigma_{13}^\infty). \tag{32}$$

The crack-tip field of an interface crack is uniquely determined by the complex SIF (32) or by its real and imaginary parts, respectively. Employing a polar coordinate system  $(\rho, \theta)$  with the origin at the right crack tip, the near-tip tractions along the bonded interface part  $(\theta = 0)$  are expressed as

$$\sigma_{33}(\rho, 0) - im_1\sigma_{13}(\rho, 0) = \frac{K_1 - im_1K_2}{\sqrt{2\pi\rho}}(\rho/l)^{i\varepsilon_1} \quad \text{for } \rho \rightarrow 0. \tag{33}$$

The corresponding near-tip expression for the discontinuity in displacement across the crack  $(\theta = \pi)$  is

$$\langle u_3(\rho) \rangle + \frac{i}{s_1} \langle u_1(\rho) \rangle = \frac{2}{s_1 t_1 \sqrt{\gamma_1}} \frac{K_1 - im_1K_2}{1 + 2i\varepsilon_1} \sqrt{\frac{\rho}{2\pi}} (\rho/l)^{i\varepsilon_1} \quad \text{for } \rho \rightarrow 0. \tag{34}$$

Using

$$(\rho/l)^{i\varepsilon_1} = \cos[\varepsilon_1 \ln(\rho/l)] + i \sin[\varepsilon_1 \ln(\rho/l)],$$

it can be seen that the asymptotic fields (33) and (34) change their sign an infinite number of times in a small neighboring area of the crack tip. This means that for the open crack model the well-known oscillating singularity is observed [Williams 1959]. It is characterized by physically unrealistic interpenetration of the two materials along the crack faces. The degree of oscillation is determined by parameter  $\varepsilon_1$ , which depends on the ratio of the stiffness characteristics of the two materials. With the definitions employed for  $\gamma_1$  and  $\varepsilon_1$ ,  $\gamma_1 > 1$  implies  $\varepsilon_1 > 0$ . For identical materials it holds that  $\gamma_1 = 1$  and  $\varepsilon_1 = 0$ . It should also be noticed that transposition of the half-planes yields a change in the sign of  $\varepsilon_1$ .

Defining the phase angle of the complex SIF as  $\psi_K = \arg(K_1 - im_1K_2)$  and taking into account that

$$K_1 - im_1K_2 = |K_1 - im_1K_2| e^{i\psi_K}, \quad 1 + 2i\varepsilon_1 = \sqrt{1 + 4\varepsilon_1^2} e^{i \arctan(2\varepsilon_1)},$$

hold true and separating real and imaginary parts of the expression (34), we have

$$\langle u_3(\rho) \rangle = \frac{2}{s_1 t_1 \sqrt{\gamma_1}} \frac{|K_1 - i m_1 K_2|}{\sqrt{1 + 4\varepsilon_1^2}} \sqrt{\frac{\rho}{2\pi}} \cos[\psi_u(\rho)] \quad \text{for } \rho \rightarrow 0, \tag{35}$$

with

$$\psi_u(\rho) = \psi_K + \varepsilon_1 \ln(\rho/l) - \arctan(2\varepsilon_1). \tag{36}$$

As the opening of the crack,  $\langle u_3(\rho) \rangle$ , oscillates, an infinite number of interpenetration zones exists, in which  $\langle u_3(\rho) \rangle < 0$ . By means of the expression (35), we can estimate the length of the interpenetration region at the crack tip. For this purpose, we identify the location of the first interpenetration point  $\rho_I$  where the crack opening  $\langle u_3(\rho) \rangle$  due to the oscillation becomes zero for the first time. As pointed out by Hills and Barber [1993], imposing  $\langle u_3(\rho) \rangle < 0$  in (35), interpenetration zones are defined by the condition  $\cos[\psi_u(\rho)] < 0$ , which results in the intervals

$$(2n - \frac{3}{2})\pi < \psi_u(\rho) < (2n - \frac{1}{2})\pi,$$

with  $n$  being any integer. Therefore, in view of (36), the interpenetration zones are characterized by the intervals

$$\rho_L < \rho < \rho_R, \tag{37}$$

where

$$\rho_L = l \exp\left\{ \frac{1}{\varepsilon_1} \left[ (2n - \frac{3}{2})\pi - \psi_K + \arctan(2\varepsilon_1) \right] \right\}, \quad \rho_R = l \exp\left\{ \frac{1}{\varepsilon_1} \left[ (2n - \frac{1}{2})\pi - \psi_K + \arctan(2\varepsilon_1) \right] \right\}.$$

Equation (37) defines an infinite sequence of interpenetration zones as  $n$  takes all integer values, positive and negative. Hills and Barber [1993] concluded that the location of the first interpenetration point  $\rho_I$  can be obtained as the largest value of  $\rho_R$  which is lower than the crack length, i.e.,

$$\rho_I = l \exp\left\{ \frac{1}{\varepsilon_1} \left[ (2n - \frac{1}{2})\pi - \psi_K + \arctan(2\varepsilon_1) \right] \right\}. \tag{38}$$

It is worth reminding that the relation (38) is valid for  $\varepsilon_1 > 0$  only. In the case  $\varepsilon_1 < 0$ , the inequalities (37) must be reversed, and therefore the location of the first interpenetration point is defined by the largest value of  $\rho_L$  which is lower than the crack length [Graciani et al. 2007].

For the open crack model, the energy release rate (ERR) at the right crack tip is defined as [Parton and Kudryavtsev 1988]

$$G = \lim_{\Delta l \rightarrow 0} \frac{1}{2\Delta l} \int_b^{b+\Delta l} \sigma_{33}(\tau, 0) \langle u_3(\tau - \Delta l) \rangle + \sigma_{13}(\tau, 0) \langle u_1(\tau - \Delta l) \rangle d\tau. \tag{39}$$

The electrical component of the energy release rate is missing since the drop of electric potential for an electrically conducting crack is zero along the entire material interface.

Substituting expressions (33) and (34) into (39), we get

$$G = -\frac{K_1^2 + m_1^2 K_2^2}{2m_1 t_1 (1 + \gamma_1)}. \tag{40}$$

In deriving (40), the identity

$$\int_0^{\Delta l} \left( \frac{\Delta l - \tau}{\tau} \right)^{(1/2)+i\varepsilon_1} d\tau = \frac{1}{2}\pi \Delta l (1 + 2i\varepsilon_1) \operatorname{sech}(\pi \varepsilon_1),$$

has been used with  $\varepsilon_1 > 0$  and  $\Delta l > 0$ .

### 5. Contact zone model

Considering the same type of loadings at infinity, following Comninou [1977], we introduce a frictionless contact zone  $a < x_1 < b$  at the right crack tip to avoid an oscillating singularity, where the position of the point  $a$  is chosen arbitrarily for the time being (Figure 2). For a such an arbitrary position of point  $a$ , we have an artificial contact zone model, which is not physically justified, but from this model the specific value of  $a$  for the realistic contact zone length in the sense of Comninou will be found. Taking into consideration only the right contact zone is justified by the fact that the left contact zone under considered loading is extremely short and its influence upon the longer right contact zone is negligibly small [Dundurs and Gdoutos 1988].

The boundary conditions at the crack faces for the considered model can be written as

$$\sigma_{13}^{\pm}(x_1, 0) = 0, \quad \sigma_{33}^{\pm}(x_1, 0) = 0 \quad \text{for } x_1 \in (-b, a), \tag{41}$$

$$\sigma_{13}^{\pm}(x_1, 0) = 0, \quad \langle u_3(x_1) \rangle = 0 \quad \text{for } x_1 \in (a, b). \tag{42}$$

Satisfying conditions (41), (42) by means of the expressions (21), (22) leads to the homogeneous combined Dirichlet–Riemann boundary value problem

$$F_1^+(x_1) + \gamma_1 F_1^-(x_1) = 0, \quad x_1 \in (-b, a), \quad \operatorname{Im} F_1^{\pm}(x_1) = 0, \quad x_1 \in (a, b). \tag{43}$$

The behavior of the function  $F_1(z)$  at infinity is determined by (27).

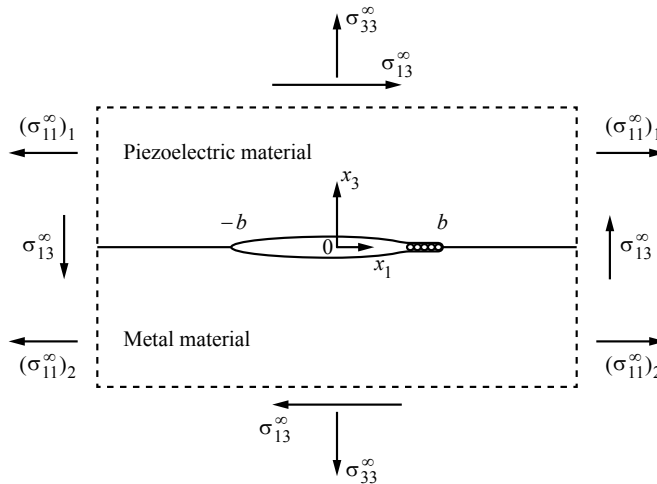


**Figure 2.** An interface crack with one contact zone subject to remote uniform mechanical loading.

Following Nakhmein and Nuller [1986] and Herrmann and Loboda [2000], the general solution of the problem (43) can be represented in the form

$$F_1(z) = P(z)X_1(z) + Q(z)X_2(z), \tag{44}$$

where

$$X_1(z) = \frac{ie^{i\theta(z)}}{\sqrt{(z+b)(z-b)}}, \quad X_2(z) = \frac{e^{i\theta(z)}}{\sqrt{(z+b)(z-a)}}, \quad \theta(z) = 2\varepsilon_1 \ln \frac{\sqrt{(b-a)(z+b)}}{\sqrt{l(z-a) + \sqrt{(a+b)(z-b)}}},$$

and  $P(z) = C_1z + C_0$ ,  $Q(z) = D_1z + D_0$  are polynomials with arbitrary real coefficients. Constants  $C_0$ ,  $C_1$ ,  $D_0$ ,  $D_1$  can be found from the condition (27) at infinity in the form

$$\begin{aligned} C_0 &= -\beta_1 D_1, & D_0 &= \beta_1 C_1 - \frac{a-b}{2} D_1, \\ C_1 &= \frac{m_1 \sigma_{13}^\infty \cos \beta - \sigma_{33}^\infty \sin \beta}{t_1(1 + \gamma_1)}, & D_1 &= \frac{\sigma_{33}^\infty \cos \beta + m_1 \sigma_{13}^\infty \sin \beta}{t_1(1 + \gamma_1)}, \end{aligned}$$

where

$$\beta = \varepsilon_1 \ln \frac{\lambda}{2(1 + \sqrt{1 - \lambda}) - \lambda}, \quad \beta_1 = \varepsilon_1 \sqrt{l(a+b)}.$$

The parameter  $\lambda = (b - a)/l$  defines the relative length of the contact zone of the crack faces and will be found later.

Substituting the formula (44) into (21), (22) and taking into account that  $F_1^+(x_1) = F_1^-(x_1)$  for  $x_1 > b$  and  $F_1^-(x_1) = -F_1^+(x_1)/\gamma_1$  for  $x_1 \in (-b, a)$ , the following expressions are obtained for the stresses and the derivatives of the displacement jumps at the material interface for  $x_1 > b$ :

$$\sigma_{33}(x_1, 0) + im_1\sigma_{13}(x_1, 0) = \frac{t_1(1 + \gamma_1) e^{i\theta(x_1)}}{\sqrt{x_1 + b}} \left[ \frac{Q(x_1)}{\sqrt{x_1 - a}} + i \frac{P(x_1)}{\sqrt{x_1 - b}} \right], \tag{45}$$

for  $x_1 \in (-b, a)$ ,

$$\langle u'_1(x_1) \rangle + is_1 \langle u'_3(x_1) \rangle = \frac{(1 + \gamma_1) e^{i\theta^*(x_1)}}{\sqrt{\gamma(x_1 + b)}} \left[ \frac{P(x_1)}{\sqrt{b - x_1}} - i \frac{Q(x_1)}{\sqrt{a - x_1}} \right]; \tag{46}$$

for  $x_1 \in (a, b)$ ,

$$\begin{aligned} \sigma_{33}(x_1, 0) &= \frac{t_1(1 + \gamma_1)P(x_1)}{\sqrt{(x_1 + b)(b - x_1)}} \left[ \sinh \tilde{\theta}(x_1) + \frac{1 - \gamma_1}{1 + \gamma_1} \cosh \tilde{\theta}(x_1) \right] \\ &\quad + \frac{t_1(1 + \gamma_1)Q(x_1)}{\sqrt{(x_1 + b)(x_1 - a)}} \left[ \cosh \tilde{\theta}(x_1) + \frac{1 - \gamma_1}{1 + \gamma_1} \sinh \tilde{\theta}(x_1) \right], \end{aligned} \tag{47}$$

$$\langle u'_1(x_1) \rangle = \frac{2}{\sqrt{x_1 + b}} \left[ \frac{P(x_1)}{\sqrt{b - x_1}} \cosh \tilde{\theta}(x_1) + \frac{Q(x_1)}{\sqrt{x_1 - a}} \sinh \tilde{\theta}(x_1) \right], \tag{48}$$

where

$$\theta^*(x_1) = 2\varepsilon_1 \ln \frac{\sqrt{(b-a)(x_1 + b)}}{\sqrt{l(a-x_1) + \sqrt{(a+b)(b-x_1)}}}, \quad \tilde{\theta}(x_1) = 2\varepsilon_1 \arctan \sqrt{\frac{(a+b)(b-x_1)}{l(x_1 - a)}}.$$

As it follows from the analysis of the formulas (45) and (47) the normal stress is limited for  $x_1 \rightarrow b + 0$ . On the other hand, the shear stress is singular for  $x_1 \rightarrow b + 0$  as well as the normal stress for  $x_1 \rightarrow a + 0$ . The stress intensity factors are introduced to characterize these singularities:

$$k_1 = \lim_{x_1 \rightarrow a+0} \sqrt{2\pi(x_1 - a)} \sigma_{33}(x_1, 0), \quad k_2 = \lim_{x_1 \rightarrow b+0} \sqrt{2\pi(x_1 - b)} \sigma_{13}(x_1, 0).$$

Using relations (45) and (47) leads to the expressions

$$\begin{aligned} k_1 &= \frac{\sqrt{2\pi l \gamma_1}}{1 + \gamma_1} \left[ \sqrt{1 - \gamma} (\sigma_{33}^\infty \cos \beta + m_1 \sigma_{13}^\infty \sin \beta) - 2\varepsilon_1 (\sigma_{33}^\infty \sin \beta - m_1 \sigma_{13}^\infty \cos \beta) \right], \\ k_2 &= -\frac{1}{m_1} \sqrt{\frac{1}{2} \pi l} \left[ \sigma_{33}^\infty \sin \beta - m_1 \sigma_{13}^\infty \cos \beta + 2\varepsilon_1 \sqrt{1 - \lambda} (\sigma_{33}^\infty \cos \beta + m_1 \sigma_{13}^\infty \sin \beta) \right]. \end{aligned} \tag{49}$$

We define the energy release rate near the right crack tip as [Parton and Kudryavtsev 1988]

$$G = \lim_{\Delta l \rightarrow 0} \frac{1}{2\Delta l} \left\{ \int_a^{a+\Delta l} \sigma_{33}(x_1, 0) \langle u_3(x_1 - \Delta l) \rangle dx_1 + \int_b^{b+\Delta l} \sigma_{13}(x_1, 0) \langle u_1(x_1 - \Delta l) \rangle dx_1 \right\}. \tag{50}$$

Substituting the asymptotic formulas for the stresses and the displacement jumps in the vicinity of the points  $a$  and  $b$  into (50) and calculating the corresponding integrals, we get

$$G = \frac{1}{2t_1} \left( \frac{1 + \gamma_1}{4s_1 \gamma_1} k_1^2 - \frac{m_1}{1 + \gamma_1} k_2^2 \right). \tag{51}$$

The obtained solution is mathematically correct for any position of the point  $a$ , and the associated interface crack model was called an artificial contact zone model [Herrmann and Loboda 2000]. However, it is physically justified if the inequalities

$$\sigma_{33}(x_1, 0) \leq 0, \quad x_1 \in (a, b), \quad \langle u_3(x_1) \rangle \geq 0, \quad x_1 \in (-b, a), \tag{52}$$

are valid. The first inequality ensures that the crack faces are closing on  $(a, b)$ , and the second one excludes their interpenetration on  $(-b, a)$  (it violates only in a very small area near the left crack tip because of oscillation, but it does not significantly influence in the vicinity of the right crack tip, as mentioned before). In this case a realistic contact zone in the sense of Comninou [1977] is present at the crack tip.

The inequalities in (52) are satisfied simultaneously in the case of a smooth closing of the crack at the point  $a$ , i.e., when  $k_1 = 0$  [Loboda 1993]. The latter condition is a necessary one for the satisfaction of the inequalities in (52) and, from (49), it leads to the transcendental equation

$$\tan \beta = \frac{\sqrt{1 - \lambda} \sigma_{33}^\infty + 2\varepsilon_1 m_1 \sigma_{13}^\infty}{2\varepsilon_1 \sigma_{33}^\infty - \sqrt{1 - \lambda} m_1 \sigma_{13}^\infty}, \tag{53}$$

with respect to the parameter  $\lambda$ . Usually (53) is solved numerically and the maximum root  $\lambda = \lambda_0$  from interval  $(0, 1)$  should be selected. For small values of  $\lambda$ , assuming  $\sqrt{1 - \lambda} \approx 1$ , we get the asymptotic formula

$$\lambda_0 = 4 \exp \left\{ -\frac{1}{\varepsilon_1} \left[ \arctan(2\varepsilon_1) - \arctan \left( \frac{m_1 \sigma_{13}^\infty}{\sigma_{33}^\infty} \right) - \pi(n - 0, 5) \right] \right\}, \tag{54}$$

where the integer  $n$  is chosen to provide  $\lambda_0$  as the maximum root of (54) in the interval  $(0, 1)$ .

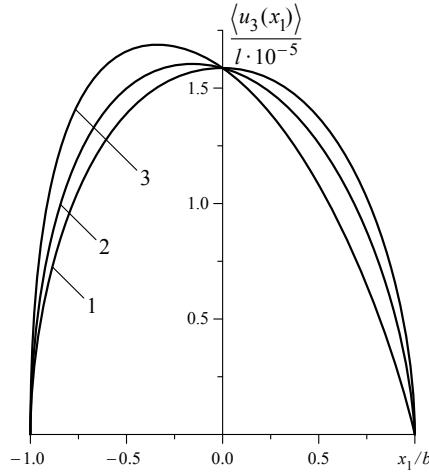


**Figure 3.** The variation of the normalized crack opening along the crack region for  $\sigma_{33}^\infty = 1$  MPa and  $\sigma_{13}^\infty / \sigma_{33}^\infty = -1$  (line 1),  $\sigma_{13}^\infty / \sigma_{33}^\infty = -20$  (line 2),  $\sigma_{13}^\infty / \sigma_{33}^\infty = -50$  (line 3).

### 6. Numerical results and discussion

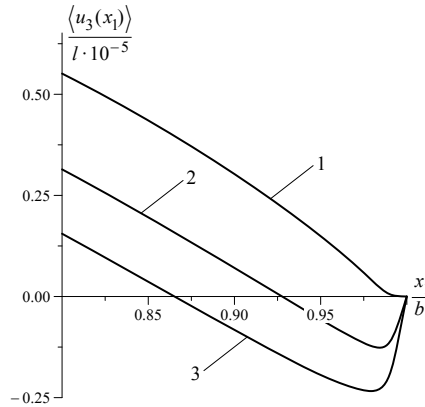
We pay our attention to the influence of the external mechanical loading on the crack opening and the stresses as well as the contact zone and interpenetration region lengths. The bimaterial consisting of piezoceramic PZT-4 [Pak 1992] (the upper material) and steel (Young’s modulus  $E = 21.0 \times 10^{10}$  N/m<sup>2</sup> and Poisson’s ratio  $\nu = 0.3$ ) (the lower one) is chosen for the numerical calculations. In the SI system of units, matrix  $\mathbf{D}$  for the piezoceramic PZT-4 has the form

$$\begin{bmatrix} 4.69302 \cdot 10^{10} i & 5.80012 \cdot 10^9 & 11.5642 \\ -5.80012 \cdot 10^9 & 4.39991 \cdot 10^{10} i & 12.3926 i \\ -11.5642 & 12.3926 i & -5.81112 \cdot 10^{-9} i \end{bmatrix}.$$

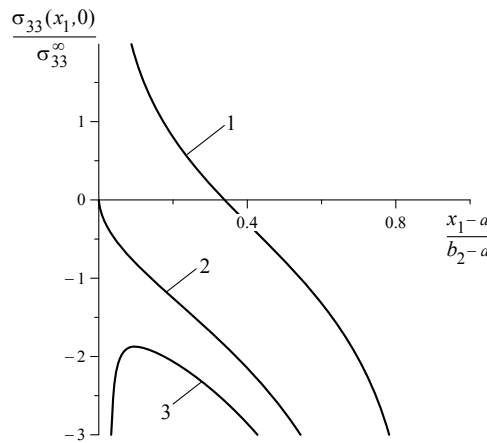
At the beginning, the variation of the normalized normal crack displacement jump (crack opening) along the crack region for the open crack model is shown in Figure 3. The graphs are presented for different shear loads  $\sigma_{13}^\infty = -1$  MPa (line 1),  $\sigma_{13}^\infty = -20$  MPa (line 2), and  $\sigma_{13}^\infty = -50$  MPa (line 3) with fixed  $\sigma_{33}^\infty = 1$  MPa. The obtained results confirm the essential influence of normal-shear loading coefficient on the crack opening.

Figure 4 shows the graph of the normalized displacement jump at the right crack tip for the open crack model. Curves 1, 2, and 3 in this figure correspond to the values  $\sigma_{13}^\infty / \sigma_{33}^\infty = -50$ ,  $\sigma_{13}^\infty / \sigma_{33}^\infty = -80$ , and  $\sigma_{13}^\infty / \sigma_{33}^\infty = -100$ , respectively. It follows from the analysis of these graphs that crack opening is negative in some areas, i.e., a physically impossible overlapping of the crack faces is observed there. If  $\sigma_{13}^\infty / \sigma_{33}^\infty = -50$  this overlapping is invisibly small although it takes place, but for  $\sigma_{13}^\infty / \sigma_{33}^\infty = -80$  it is quite noticeable and for  $\sigma_{13}^\infty / \sigma_{33}^\infty = -100$  the overlapping covers one tenth of the crack length. It is clear that in such cases the open crack model is not adequate to reality and the contact zone model should be used.

The distribution of the normalized normal stress  $\sigma_{33}(x_1, 0) / \sigma_{33}^\infty$  in the contact zone  $x_1 \in (a, b)$  for  $\sigma_{33}^\infty = 1$  MPa,  $\sigma_{13}^\infty / \sigma_{33}^\infty = -70$  and different values of the relative contact zone length  $\lambda$  is shown in



**Figure 4.** The variation of the normalized crack opening along the near-crack tip region for  $\sigma_{33}^\infty = 1$  MPa and  $\sigma_{13}^\infty/\sigma_{33}^\infty = -50$  (line 1),  $\sigma_{13}^\infty/\sigma_{33}^\infty = -80$  (line 2),  $\sigma_{13}^\infty/\sigma_{33}^\infty = -100$  (line 3).



**Figure 5.** Variation of the normalized normal stress  $\sigma_{33}(x_1, 0)/\sigma_{33}^\infty$  in the contact zone  $(a, b)$  for  $\sigma_{33}^\infty = 1$  MPa,  $\sigma_{13}^\infty/\sigma_{33}^\infty = -70$ , and  $\lambda = 0.03$  (line 1),  $\lambda = \lambda_0 \approx 0.01238$  (line 2),  $\lambda = 0.001$  (line 3).

**Figure 5.** Curve 1 corresponds to  $\lambda = 0.03$  ( $\lambda > \lambda_0$ ), curve 2 to  $\lambda = \lambda_0 \approx 0.01238$ , and curve 3 to  $\lambda = 0.01$  ( $\lambda < \lambda_0$ ). It is seen that for  $\lambda > \lambda_0$ , normal stress is tensile in most parts of the interval  $(a, b)$  and is compressive only near the point  $b$ . A decrease of  $\lambda$  leads to an increase of the compressive stress field zone. For  $\lambda \leq \lambda_0$ , the normal stress becomes negative throughout the interval  $(a, b)$ . Only for  $\lambda = \lambda_0$  the stress  $\sigma_{33}(x_1, 0)$  at the point  $a$  becomes equal to zero. This means that for  $\lambda = \lambda_0$ , the crack faces are compressed against each other in the entire interval  $(a, b)$  and their closure in point  $a$  is smooth.

**Figure 6** shows the normalized crack opening  $\langle u_3(x_1) \rangle / l$  in the left neighboring area of the point  $a$  for the same materials and loads, as in **Figure 5**. Curve 1 corresponds to  $\lambda = 0.03$  ( $\lambda > \lambda_0$ ), curve 2 to  $\lambda = \lambda_0 \approx 0.01238$ , and curve 3 to  $\lambda = 0.001$  ( $\lambda < \lambda_0$ ). It follows from the analysis of the above results that for  $\lambda \geq \lambda_0$  the second inequality in (52) is satisfied for all  $x_1 \in (-b, a)$ , except  $\lim_{x_1 \rightarrow a-0} \langle u_3'(x_1) \rangle \rightarrow 0$ ,

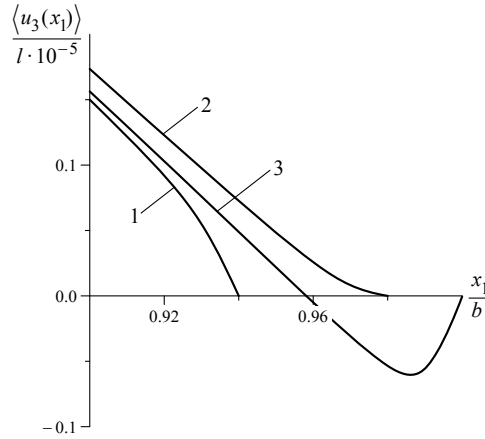


**Figure 6.** Variation of the normalized crack opening  $\langle u_3(x_1) \rangle / l$  in the left neighboring area of the point  $a$  for  $\sigma_{33}^\infty = 1$  MPa,  $\sigma_{13}^\infty / \sigma_{33}^\infty = -70$ , and  $\lambda = 0.03$  (line 1),  $\lambda = \lambda_0 \approx 0.01238$  (line 2),  $\lambda = 0.001$  (line 3).

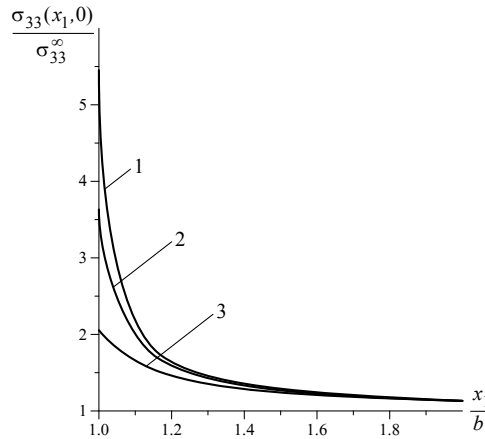


**Figure 7.** Variation of the normalized normal stress  $\sigma_{33}(x_1, 0) / \sigma_{33}^\infty$  for the contact zone model at the crack continuation for  $\sigma_{33}^\infty = 1$  MPa and  $\sigma_{13}^\infty / \sigma_{33}^\infty = -40$  (line 1),  $\sigma_{13}^\infty / \sigma_{33}^\infty = -50$  (line 2),  $\sigma_{13}^\infty / \sigma_{33}^\infty = -80$  (line 3).

and equality  $\langle u_3'(a) \rangle = 0$  holds true only for  $\lambda = \lambda_0$ . On the other hand, if  $\lambda < \lambda_0$ , physically incorrect overlapping of the crack faces is observed, which increases with  $\lambda$  decreasing. Thus, the results presented in Figure 5 and Figure 6 numerically confirm the fact that the inequalities in (52) are satisfied only for  $\lambda = \lambda_0$ .

The results of the calculations of the normalized normal stress  $\sigma_{33}(x_1, 0) / \sigma_{33}^\infty$  at the crack continuations are shown in Figure 7. Curves 1, 2, and 3 in this figure correspond to the values  $\sigma_{13}^\infty / \sigma_{33}^\infty = -40$ ,  $\sigma_{13}^\infty / \sigma_{33}^\infty = -50$ , and  $\sigma_{13}^\infty / \sigma_{33}^\infty = -80$ , respectively. These results demonstrate that, although the normal stress  $\sigma_{33}(x_1, 0)$  is not singular in the right neighborhood of the point  $b$ , its value remains very high in this region and can contribute crack propagation.

$\sigma_{13}^{\infty}/\sigma_{33}^{\infty}$	$\rho_I/l$	$\lambda_0$	$G/(l\sigma_{33}^{\infty})$
-10	$4.08058 \cdot 10^{-12}$	$2.20907 \cdot 10^{-12}$	$1.20334 \cdot 10^{-3}$
-20	$1.95214 \cdot 10^{-6}$	$1.05682 \cdot 10^{-6}$	$4.77593 \cdot 10^{-3}$
-30	$1.55536 \cdot 10^{-4}$	$8.41908 \cdot 10^{-5}$	$1.07303 \cdot 10^{-2}$
-40	$1.39120 \cdot 10^{-3}$	$7.52293 \cdot 10^{-4}$	$1.90663 \cdot 10^{-2}$
-50	$5.18241 \cdot 10^{-3}$	$2.79381 \cdot 10^{-3}$	$2.97841 \cdot 10^{-2}$
-60	$1.24555 \cdot 10^{-2}$	$6.67549 \cdot 10^{-3}$	$4.28836 \cdot 10^{-2}$
-70	$2.33029 \cdot 10^{-2}$	$1.23814 \cdot 10^{-2}$	$5.83648 \cdot 10^{-2}$
-80	$3.72787 \cdot 10^{-2}$	$1.95898 \cdot 10^{-2}$	$7.62278 \cdot 10^{-2}$

**Table 1.** The variation of the relative interpenetration region length  $\rho_I/l$ , the relative contact zone length  $\lambda_0$ , and the normalized energy release rate  $G/(l\sigma_{33}^{\infty})$  with respect to different shear loads  $\sigma_{13}^{\infty}/\sigma_{33}^{\infty}$  for  $\sigma_{33}^{\infty} = 1$  MPa.

In Table 1, the magnitudes of the relative interpenetration region length  $\rho_I/l$ , the relative contact zone length  $\lambda_0$  and the energy release rate  $G$  for different values of the shear loads are presented. It can be seen that all these values increase with the increase of magnitude of the applied shear load. In the absence of shear stress, the contact zone and interpenetration region lengths for piezoelectric-metal structures are several orders less than the characteristic size of the crack. However, for an essential shear field they become longer and even comparable with the crack length.

Comparing the results shown in Table 1, we can note that under the same loads the relative length of the material interpenetration region is always longer than the relative length of the realistic contact zone. This finding can be useful for the prediction of the first approximation for the realistic contact zone length, which can be refined later by an iterative procedure.

Carrying out a similar analysis for  $\sigma_{13}(x_1, 0)$  for  $x_1 \rightarrow b+0$ , one can see that the size of the area in the vicinity of the crack tip, where the stress changes its sign an infinite number of times, is approximately equal to  $\rho_I$ .

## 7. Conclusion

An interface crack between a piezoelectric material and a conducting isotropic elastic material under the action of a mechanical loading has been considered. By using a hybrid complex variable method which combines the Stroh formalism of piezoelectric materials with the Muskhelishvili formalism of isotropic elastic materials, the stresses and the derivatives of the displacement jumps via sectionally holomorphic functions have been presented. On the base of these representations, the exact analytical solutions for two interface crack models — the open crack one and the contact zone one — have been found. Furthermore, the explicit expressions of the crack tip ERR and the crack tip SIF have been obtained when the piezoelectric-metal bimaterial is subjected to the mechanical loading at infinity.

The present investigation shows that the structure of the singular fields near the conducting interface crack tip within the framework of the open crack model consists of an oscillating singularity, which is similar to that in the linear elastic dissimilar anisotropic materials but quite different from that under the impermeable crack assumption. It can be concluded that the electric boundary condition along

an interface crack in piezoelectric-metal bimetals exerts significant influence on the structure of the singularity of the near-tip fields. An oscillating singularity is characterized by physically unrealistic interpenetration of the two materials along the crack faces. The degree of oscillation is determined by parameter  $\varepsilon_1$ , which depends on the ratio of the stiffness characteristics of the two materials. The zone of crack face interpenetrations at the crack tip has been investigated and, in particular, the distance between the point of first interpenetration and the crack tip in the open crack model solution has been estimated.

The contact zone model in Comninou's sense has been derived as a particular case of the obtained solution within the framework of the artificial contact zone model. A simple transcendental equation and corresponding asymptotic formulas have been found for the determination of the realistic contact zone length. It is shown that at the same loads the relative length of the material interpenetration region is always longer than the relative length of the realistic contact area. This finding can be useful for the prediction of the first approximation for the realistic contact zone length, which can be refined later by an iterative procedure.

### Acknowledgments

Part of this work was executed during a stay of Govorukha at Karlsruhe Institute of Technology (KIT). The authors gratefully acknowledge the support from KIT by funding a guest stay of Govorukha.

### References

- [Bakirov 2004] V. F. Bakirov, "Integral relations for the problem of a crack on a piezoelectric-conductor interface", *Mech. Solids* **39**:6 (2004), 99–115.
- [Bakirov and Kim 2009] V. F. Bakirov and T.-W. Kim, "Analysis of a crack at the piezoceramic-metal interface and estimates of adhesion fracture energy", *Int. J. Eng. Sci.* **47**:7-8 (2009), 793–804.
- [Comninou 1977] M. Comninou, "The interface crack", *J. Appl. Mech. (ASME)* **44**:4 (1977), 631–636.
- [Dundurs and Gautesen 1988] J. Dundurs and A. K. Gautesen, "An opportunistic analysis of the interface crack", *Int. J. Fract.* **36**:2 (1988), 151–159.
- [Eshelby et al. 1953] J. D. Eshelby, W. T. Read, and W. Shockley, "Anisotropic elasticity with applications to dislocation theory", *Acta Metall.* **1**:3 (1953), 251–259.
- [Govorukha and Loboda 2000] V. B. Govorukha and V. V. Loboda, "Contact zone models for an interface crack in a piezoelectric material", *Acta Mech.* **140**:3-4 (2000), 233–246.
- [Govorukha et al. 2016] V. Govorukha, M. Kamlah, V. Loboda, and Y. Lapusta, "Interface cracks in piezoelectric materials", *Smart Mater. Struct.* **25**:2 (2016), 023001.
- [Graciani et al. 2007] E. Graciani, V. Mantič, and F. Paris, "On the estimation of the first interpenetration point in the open model of interface cracks", *Int. J. Fract.* **143**:3 (2007), 287–290.
- [Herrmann and Loboda 2000] K. P. Herrmann and V. V. Loboda, "Fracture-mechanical assessment of electrically permeable interface cracks in piezoelectric bimetals by considerations of various contact zone models", *Arch. Appl. Mech.* **70**:1-3 (2000), 127–143.
- [Hills and Barber 1993] D. A. Hills and J. R. Barber, "Interface cracks", *Int. J. Mech. Sci.* **35**:1 (1993), 27–37.
- [Kudriavtsev et al. 1975a] B. A. Kudriavtsev, V. Z. Parton, and V. I. Rakitin, "Fracture mechanics of piezoelectric materials: axisymmetric crack on the boundary with a conductor", *J. Appl. Math. Mech.* **39**:2 (1975), 328–338.
- [Kudriavtsev et al. 1975b] B. A. Kudriavtsev, V. Z. Parton, and V. I. Rakitin, "Fracture mechanics of piezoelectric materials: rectilinear tunnel crack on the boundary with a conductor", *J. Appl. Math. Mech.* **39**:1 (1975), 136–146.
- [Li and Chen 2007] Q. Li and Y. Chen, "Analysis of crack-tip singularities for an interfacial permeable crack in metal/piezoelectric bimetals", *Acta Mech. Solida Sin.* **20**:3 (2007), 247–257.

- [Li and Chen 2009] Q. Li and Y. H. Chen, “The Coulombic traction on the surfaces of an interface crack in dielectric/piezoelectric or metal/piezoelectric bimetals”, *Acta Mech.* **202**:1-4 (2009), 111–126.
- [Liu and Hsia 2003] M. Liu and K. J. Hsia, “Interfacial cracks between piezoelectric and elastic materials under in-plane electric loading”, *J. Mech. Phys. Solids* **51**:5 (2003), 921–944.
- [Loboda 1993] V. V. Loboda, “The quasi-invariant in the theory of interface crack”, *Eng. Fract. Mech.* **44**:4 (1993), 573–580.
- [Muskhelishvili 1953] N. I. Muskhelishvili, *Some basic problems of mathematical theory of elasticity*, Noordhoff Publishers, Groningen, 1953.
- [Nakhmein and Nuller 1986] E. L. Nakhmein and B. M. Nuller, “Contact between an elastic half-plane and a partly separated stamp”, *J. Appl. Math. Mech.* **50**:4 (1986), 507–515.
- [Ou and Chen 2004] Z. C. Ou and Y. H. Chen, “Near-tip stress fields and intensity factors for an interface crack in metal/piezoelectric bimetals”, *Int. J. Eng. Sci.* **42**:13-14 (2004), 1407–1438.
- [Pak 1992] Y. E. Pak, “Linear electro-elastic fracture mechanics of piezoelectric materials”, *Int. J. Fract.* **54**:1 (1992), 79–100.
- [Parton 1976] V. Z. Parton, “Fracture mechanics of piezoelectric materials”, *Acta Astronaut.* **3**:9-10 (1976), 671–683.
- [Parton and Kudryavtsev 1988] V. Z. Parton and B. A. Kudryavtsev, *Electromagnetoelasticity*, Gordon and Breach Science Publishers, New York, 1988.
- [Pritchard et al. 2001] J. Pritchard, C. R. Bowen, and F. Lowrie, “Multilayer actuators: review”, *Br. Ceram. Trans.* **100**:6 (2001), 265–273.
- [Rice 1988] J. R. Rice, “Elastic fracture mechanics concepts for interfacial cracks”, *J. Appl. Mech. (ASME)* **55**:1 (1988), 98–103.
- [Ru 2008] C. Q. Ru, “A hybrid complex-variable solution for piezoelectric/isotropic elastic interfacial cracks”, *Int. J. Fract.* **152**:2 (2008), 169–178.
- [Stroh 1958] A. N. Stroh, “Dislocation and crack in anisotropic elasticity”, *Phil. Mag.* **3**:30 (1958), 625–646.
- [Suo et al. 1992] Z. Suo, C.-M. Kuo, D. M. Barnett, and J. R. Willis, “Fracture mechanics for piezoelectric ceramics”, *J. Mech. Phys. Solids* **40**:4 (1992), 739–765.
- [Ting and Chou 1981] T. C. T. Ting and S. C. Chou, “Edge singularities in anisotropic composites”, *Int. J. Solids Struct.* **17**:11 (1981), 1057–1068.
- [Williams 1959] M. L. Williams, “The stresses around a fault or cracks in dissimilar media”, *Bull. Seismol. Soc. Am.* **49**:2 (1959), 199–204.
- [Zhang and Gao 2004] T. Y. Zhang and C. F. Gao, “Fracture behaviors of piezoelectric materials”, *Theor. Appl. Fract. Mech.* **41**:1-3 (2004), 339–379.

Received 7 Aug 2018. Revised 9 Nov 2018. Accepted 15 Nov 2018.

VOLODYMYR GOVORUKHA: [govorukhavb@yahoo.com](mailto:govorukhavb@yahoo.com)

Department of Computational Mathematics, Oles Honchar Dnipro National University, Dnipro, Ukraine

MARC KAMLAH: [marc.kamlah@kit.edu](mailto:marc.kamlah@kit.edu)

Institute of Applied Materials, Karlsruhe Institute of Technology, Eggenstein-Leopoldshafen, Germany

# JOURNAL OF MECHANICS OF MATERIALS AND STRUCTURES

[msp.org/jomms](http://msp.org/jomms)

Founded by Charles R. Steele and Marie-Louise Steele

## EDITORIAL BOARD

ADAIR R. AGUIAR	University of São Paulo at São Carlos, Brazil
KATIA BERTOLDI	Harvard University, USA
DAVIDE BIGONI	University of Trento, Italy
MAENGHYO CHO	Seoul National University, Korea
HUILING DUAN	Beijing University
YIBIN FU	Keele University, UK
IWONA JASIUK	University of Illinois at Urbana-Champaign, USA
DENNIS KOCHMANN	ETH Zurich
MITSUTOSHI KURODA	Yamagata University, Japan
CHEE W. LIM	City University of Hong Kong
ZISHUN LIU	Xi'an Jiaotong University, China
THOMAS J. PENCE	Michigan State University, USA
GIANNI ROYER-CARFAGNI	Università degli studi di Parma, Italy
DAVID STEIGMANN	University of California at Berkeley, USA
PAUL STEINMANN	Friedrich-Alexander-Universität Erlangen-Nürnberg, Germany
KENJIRO TERADA	Tohoku University, Japan

## ADVISORY BOARD

J. P. CARTER	University of Sydney, Australia
D. H. HODGES	Georgia Institute of Technology, USA
J. HUTCHINSON	Harvard University, USA
D. PAMPLONA	Universidade Católica do Rio de Janeiro, Brazil
M. B. RUBIN	Technion, Haifa, Israel

**PRODUCTION** [production@msp.org](mailto:production@msp.org)

SILVIO LEVY Scientific Editor

---

See [msp.org/jomms](http://msp.org/jomms) for submission guidelines.

JoMMS (ISSN 1559-3959) at Mathematical Sciences Publishers, 798 Evans Hall #6840, c/o University of California, Berkeley, CA 94720-3840, is published in 10 issues a year. The subscription price for 2018 is US \$615/year for the electronic version, and \$775/year (+\$60, if shipping outside the US) for print and electronic. Subscriptions, requests for back issues, and changes of address should be sent to MSP.

---

JoMMS peer-review and production is managed by EditFLOW<sup>®</sup> from Mathematical Sciences Publishers.

PUBLISHED BY

 **mathematical sciences publishers**  
nonprofit scientific publishing

<http://msp.org/>

© 2018 Mathematical Sciences Publishers

- Prediction of springback and residual stress of a beam/plate subjected to three-point bending**      **QUANG KHOA DANG, PEI-LUN CHANG, SHIH-KANG KUO and DUNG-AN WANG**    **421**
- Characterization of CNT properties using space-frame structure**      **MUHAMMAD ARIF and JACOB MUTHU**    **443**
- Analytical approach to the problem of an auxetic layer under a spatially periodic load**      **HENRYK KAMIŃSKI and PAWEŁ FRITZKOWSKI**    **463**
- Stability and nonplanar postbuckling behavior of current-carrying microwires in a longitudinal magnetic field**      **YUANZHUO HONG, LIN WANG and HU-LIANG DAI**    **481**
- Three-dimensional Trefftz computational grains for the micromechanical modeling of heterogeneous media with coated spherical inclusions**      **GUANNAN WANG, LEITING DONG, JUNBO WANG and SATYA N. ATLURI**    **505**
- Uniform stress resultants inside two nonelliptical inhomogeneities in isotropic laminated plates**      **XU WANG, LIANG CHEN and PETER SCHIAVONE**    **531**
- An analytical solution for heat flux distribution of cylindrically orthotropic fiber reinforced composites with surface effect**      **JUNHUA XIAO, YAOLING XU and FUCHENG ZHANG**    **543**
- Strain gradient fracture of a mode III crack in an elastic layer on a substrate**      **JINE LI and BAOLIN WANG**    **555**
- Growth-induced instabilities of an elastic film on a viscoelastic substrate: analytical solution and computational approach via eigenvalue analysis**      **IMAN VALIZADEH, PAUL STEINMANN and ALI JAVILI**    **571**
- Application of the hybrid complex variable method to the analysis of a crack at a piezoelectric-metal interface**      **VOLODYMYR GOVORUKHA and MARC KAMLAH**    **587**